Spectroscopic study of the $TbAl_3(BO_3)_4$ single crystal: Raman and luminescence spectroscopy

A. V. Peschanskii and A. Yu. Glamazda

1B. Verkin Institute for Low Temperature Physics and Engineering of the National Academy of Sciences of Ukraine, Kharkov 61103, Ukraine
E-mail: peschansky@ilt.kharkov.ua

I. A. Gudim

2L. V. Kirensky Institute of Physics, Siberian Branch of RAS, Krasnoyarsk, 660036, Russia

The vibrational and luminescence properties of the $TbAl_3(BO_3)_4$ single crystal were studied in the temperature range of 5–300 K. Raman spectra of the single crystal revealed 5 of 7 A_1 and all E phonon modes predicted by the group-theory analysis. The splitting energy between the LO and TO components of polar E phonons is determined. A group of intense bands associated with the $^5D_4 \rightarrow {}^7F_0$ electronic transition was observed in the energy range of 14520–14680 cm^{-1} of the luminescence spectra. The intensity of these bands decreases upon heating. At the same time, the bands which can be assigned with $^5D_4 \rightarrow {}^7F_6$, $^5D_4 \rightarrow {}^7F_5$, and $^5D_4 \rightarrow {}^7F_4$ transitions were revealed in luminescence spectra at room temperature. The intensity of these bands is comparable to the intensity of the Raman spectrum of $TbAl_3(BO_3)_4$. The observation of luminescence from the $^5D_4$ multiplet (20600–20750 cm^{-1}) upon excitation at $\lambda_{exc} = 632.8$ nm (15803 cm^{-1}) and $\lambda_{exc} = 532$ nm (18797 cm^{-1}) indicates strong nonlinear properties of the studied crystal. The structure of the main $^7F_6$ multiplet of Tb^{+3} in the $TbAl_3(BO_3)_4$ single crystal has been studied at 5 K by Raman spectroscopy. The energies of the electronic levels of $^7F_6$ and $^5D_4$ multiplets were determined from the luminescence spectra measured at 300 K.

Keywords: $TbAl_3(BO_3)_4$, vibrational spectrum, electronic transitions, Raman spectroscopy, luminescence.

1. Introduction

In recent years, the physical properties of rare-earth aluminoborates $RAl_3(BO_3)_4$ (R is the yttrium or a rare-earth ion) have been actively studied. The interest in these crystals is caused by their nonlinear optical properties, which, combined with their high chemical and mechanical strength, make it possible to use them for frequency doubling, laser, and other devices. Yttrium and gadolinium aluminoborates with the addition of Nd are used in optoelectronics and development of mini-lasers [1–3].

$TbAl_3(BO_3)_4$ is one of the most studied crystals of this family. The transition to a magnetically ordered state was found at $T_C = 0.68$ K in $TbAl_3(BO_3)_4$ [4]. The rotational magnetocaloric effect was also observed in $TbAl_3(BO_3)_4$ [5]. The energies of the electronic levels of Tb^{3+} in the range up to 20750 cm^{-1} were determined by analysis of the luminescence spectra of this crystal taken at 77 K [6]. The energy scheme of Tb^{3+} levels in the range of 0–28850 cm^{-1} was determined by the analysis of luminescence and absorption spectra at 77 K [7].

There are few works in the literature on the study of phonon spectra in this class of crystals. The transmission spectra of powders were studied for all aluminoborates at room temperature [8]. The assignment of rare-earth aluminoborates to different space groups was carried out by IR spectroscopy [8]. $Pr_xY_{1-x}Al_3(BO_3)_4$ [9] and $YAl_3(BO_3)_4$ [10] were studied by Raman spectroscopy but complete information on the phonon spectrum is missing. Raman spectroscopy is a high sensitive and informative method that allows to reveal the local crystal distortions, defects and impurities and probe the phonon, electronic and magnetic excitations simultaneously. It motivated us for studying the $TbAl_3(BO_3)_4$ single crystal in the present work. The aim of which was to study the phonon modes and the spectrum of low-energy electronic excitations of Tb^{3+} at different temperatures.

2. Samples and measurement techniques

Studies were performed on the $TbAl_3(BO_3)_4$ single crystal of good optical quality grown from a molten solution based on bismuth trimolybdate as described in [11].

The sample was cut in a cuboidal shape of 3.75×2.81×4.1 mm with the faces thoroughly polished. The edges were parallel to the axes $Z \parallel C_3$, $X \parallel C_2$ and $Y \perp Z, X$. Orientation was carried out using the crystal habit and verified using the x-ray technique. A sample quality check was performed using a polarizing microscope. The orientation of the C_3 axis was within 1°.

Raman study was performed in the 90° configuration. Raman spectra were taken upon excitation at $\lambda_{exc} = 632.8$ nm (30 mW) of He–Ne laser and $\lambda_{exc} = 532$ nm (36 mW) of solid-state Nd:YAG laser. The scattered light was analyzed by a double monochromator Ramanor U-1000 and detected with a cooled photomultiplier RCA 31034 in photon-counting mode. The sample was mounted into an optical cryostat in helium vapor with a temperature range of 5–300 K.

Raman spectra are presented in the standard notation $k(ij)q$, where k and q are the propagation directions of the incident and scattered light with the electric vector **e** along i and j, respectively. ZZ, XY, etc., notations correspond to specific components of the scattering tensor.

The crystal structure of $TbAl_3(BO_3)_4$ is characterized by the spatial group $R32$ (D_3^7) [12] and presented in Fig. 1. The structure of the crystal can be represented in the form of layers perpendicular to the crystallographic axis c and consisting of distorted TbO_6 prisms, AlO_6 octahedra, and two types of BO_3 groups. The AlO_6 octahedra are connected by the edges in such a way that they form one-dimensional mutually independent helical chains parallel to the c axis. Al^{3+} in the AlO_6 octahedra are surrounded by three types of oxygen atoms and they occupy the positions with the C_2 point symmetry group. Tb^{3+} in TbO_6 prisms are surrounded by six oxygen atoms and are located in positions with the D_3 point symmetry group. 12 anions $(BO_3)^{3-}$ in the unit cell could be separated into two groups. In the bigger one, nine $B(2)O_3$ are isosceles triangles with the C_2 symmetry axis parallel to ab plane. In the smaller group, each of three $B(1)O_3$ is an equilateral triangle and has an axis of symmetry C_3 parallel to the c axis. The planes of triangles $B(1)O_3$ are perpendicular to the c axis and the planes of triangles $B(2)O_3$ only slightly deviate from the perpendicular to the c axis.
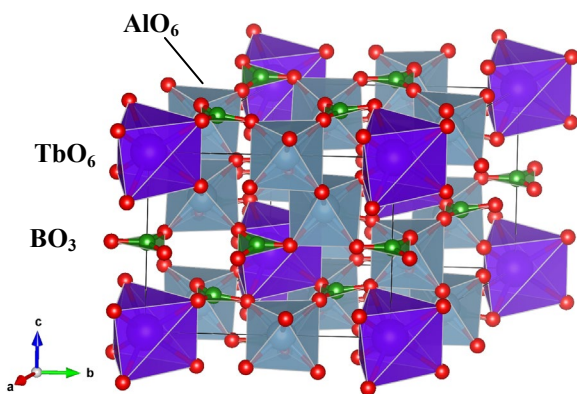
The primitive cell contains one formula unit. Group-theory analysis of the vibrational excitations in rare-earth borates has been described in [8, 13]. The lattice vibrations are described with $\Gamma_{vibr} = 7A_1 + 13A_2 + 20E$ symmetry types, including the acoustic ones $\Gamma_{ac} = A_2 + E$. It follows that $7A_1$ and doubly degenerate polar $19E$ modes are Raman-active and $12A_2 + 19E$ modes are IR-active. The non-zero components of the scattering tensor for the above setting have the form: A_1 — XX, YY, ZZ; E — $XX, YY, YZ, ZY, XY, YX, XZ, ZX$ [14]. The vibrational modes can be divided into the external $\Gamma_{ext} = 3A_1 + 8A_2 + 11E$ and internal vibrations of the BO_3 group $\Gamma_{int} = 4A_1 + 4A_2 + 8E$.

3. Experimental results and discussion

3.1. Analysis of phonon spectra of $TbAl_3(BO_3)_4$

Figure 2 shows the polarized Raman spectra of $TbAl_3(BO_3)_4$ taken at 5 K. The spectra with the ZZ component of the Raman scattering tensor allow to unambiguously identify A_1 modes, while those with off-diagonal components help to separate E modes. Spectra with XX and YY components contain both A_1 and E modes. As has been shown in previous works [13, 15, 16], for this class of compounds, the polar E modes split into TO and LO components. For Raman spectra with $\theta = 90°$ (where θ is the angle between the phonon propagation direction and the third-order axis), TO and LO components are observed simultaneously [see the presented spectra in Fig. 2 which are in polarization geometries $Y(XY)X$, $Y(XZ)X$, $Y(ZY)X$]. To separate the TO and LO components in this work, we used the sample alignment, in which the scattered light was recorded at an angle $\theta = 45°$ to the C_3 axis. Then, either only TO or LO component is observed in Raman spectra [see the presented spectra in Fig. 2 which are in $Z(YY)X$, $Z(XY)X$, $Z(XZ)X$, and $Z(YZ)X$ polarization geometries]. In contrast to Raman spectra recorded at $\theta = 90°$, the spectra measured at $\theta = 45°$ are partially polarized. This is due to

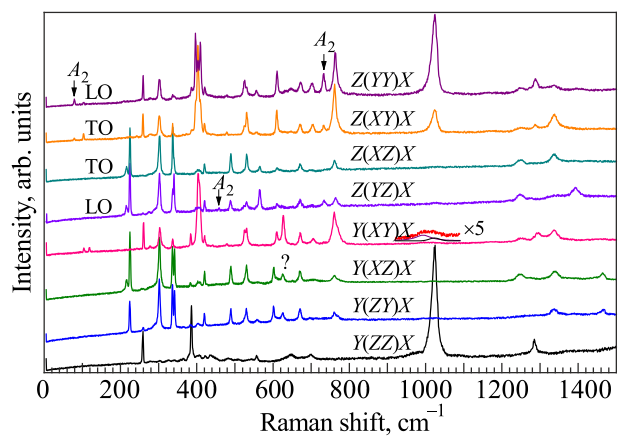*Fig. 1.* (Color online) The crystal structure of $TbAl_3(BO_3)_4$.

Fig. 2. Raman spectra of the $TbAl_3(BO_3)_4$ single crystal at 5 K in the different polarization geometries; $\lambda_{exc} = 532$ nm (36 mW); the spectral resolution of 3.0 cm^{-1}.

the fact that when exciting radiation propagates along the *Z* axis the linearly polarized light becomes elliptical. It induces a mixing of spectra with the *YY* and *XY*, *XZ* and *YZ* components of the scattering tensor.

It should also be noted that for θ = 45°, the LO component is usually shifted to lower energies by half the value of the energy difference between the TO and LO components. This has been described in more detail in our paper for the TbFe$_3$(BO$_3$)$_4$ crystal [15]. The example of the separation into TO and LO components and shifting the LO component in the θ = 45° geometry is most clearly seen in Fig. 2 for the highest frequency *E* mode.

The *A$_2$* modes are forbidden in Raman spectra at θ = 0° and 90°. The observation of inactive *A$_2$* polar excitations due to their interaction with active *E* modes in geometry at θ = 45° was shown earlier for α-quartz [17, 18]. These modes are observed in LO components and are marked with arrows in Fig. 2. Previously, *A$_2$* modes were observed in the Raman spectrum in terbium [15] and samarium [16] ferroborates.

The results of the fitting of the phonon spectra and the assignments of the lines to external and internal vibrations of the BO$_3$ group are shown in Tables 1 and 2, respectively. The error in determining the energies was no more than ± 0.5 cm^{-1}. Tables 1 and 2 show the energies of the phonon modes in isostructural TbFe$_3$(BO$_3$)$_4$ [15] and the data

obtained from the analysis of the IR transmission spectra of the TbAl$_3$(BO$_3$)$_4$ powder [8]. In the latter case, the *A$_2$* and *E* modes were observed simultaneously. The results obtained in our work can be used to interpret the transmission spectra presented in [8] and to identify the *E* modes. The exception was two *E* modes with energies of 376 and 511 cm^{-1} marked with questions in Table 1. Their frequencies are quite different from Raman data and, perhaps, these bands can be identified with the *A$_2$* vibrations. As can be seen from Tables 1 and 2, the Raman spectrum contains 5*A$_1$* + 19*E* vibrational modes of 7*A$_1$* + 19*E* predicted by the group-theory analysis. 3*A$_1$* + 11*E* can be associated with external and 2*A$_1$* (of 4*A$_1$*) + 8*E* with internal vibrations of them.

The ratio of frequencies associated with *A$_1$*, *A$_2$*, and *E* vibrational modes in isostructural TbAl$_3$(BO$_3$)$_4$ and TbFe$_3$(BO$_3$)$_4$ crystals [15] is added to Tables 1 and 2. As can be seen from Table 1, when the iron ion is replaced by an aluminum ion in the TbM$_3$(BO$_3$)$_4$ (M = Al, Fe) crystal, the frequency position of the external vibrational modes increases by a factor of 1.180–1.434. At the same time, for internal vibrational modes of the BO$_3$ group, this shift is from 1.032 to 1.063 times (Table 2). On the one hand, this is associated with a change in the lattice parameters upon the substitution of aluminum for iron (*a* = 9.5466 Å, *c* = 7.5704 Å, *V* = 597.51 Å^3 for TbFe$_3$(BO$_3$)$_4$ [19] and *a* = 9.2992 Å, *c* = 7.2588 Å, *V* = 543.61 Å^3 for TbAl$_3$(BO$_3$)$_4$ [12]). On the other hand, such a significant frequency shift indicates that the BO$_3$ group can be considered "rigid" only in the roughest approximation. As a rule, when metals are replaced in other classes of compounds, due to a change in

Table 1. The comparative analysis of the energy values (cm^{-1}) of the observed *A$_1$*, *A$_2$*, and *E* external vibrational modes in the TbAl$_3$(BO$_3$)$_4$ single crystal at 5 K and the literature data

TbAl$_3$(BO$_3$)$_4$, present work, 5 K		TbFe$_3$(BO$_3$)$_4$ [15], 300 K		ν$_{TbAl}$/ν$_{TbFe}$	IR [8], 300 K
A$_1$		*A$_1$*			
259.1		180.6		1.434	
385.7		308.2		1.251	
557.2		476.0		1.171	
A$_2$ (θ = 45°)		*A$_2$* (θ = 45°)			
79.0		60.5		1.306	80
458.5		372.6		1.231	462
E$_{TO}$	*E$_{LO}$*	*E$_{TO}$*	*E$_{LO}$*		
103.3	118.2	84.2	93.6	1.246	108
224.7		159.9		1.405	223
259.2	260.5	197.1	198.3	1.315	258
302.2		230.4		1.311	302
336.7	341.8	269.4		1.259	338
384.4	396.8	273.5	289.0	1.389	376?
403.1	409.7	315.4	330.4	1.259	401
420.5		350.7	355.8	1.191	
489.0		394.2		1.240	492
525.0		445.0		1.180	511?
530.0	601.5		489.0	1.230	546

Table 2. The comparative analysis of the energy values (cm^{-1}) of the observed *A$_1$*, *A$_2$*, and *E* internal vibrational modes in the TbAl$_3$(BO$_3$)$_4$ single crystal at 5 K and the literature data

TbAl$_3$(BO$_3$)$_4$, present work, 5 K		TbFe$_3$(BO$_3$)$_4$ [15], 300 K		ν$_{TbAl}$/ν$_{TbFe}$	IR [8], 300 K
A$_1$		*A$_1$*			
–		637.5			
–		959			
1023.3		989		1.037	
1285.3		1234.5		1.041	
A$_2$ (θ = 45°)		*A$_2$* (θ = 45°)			
732.7		709.5		1.033	731
E$_{TO}$	*E$_{LO}$*	*E$_{TO}$*	*E$_{LO}$*		
612.5		580.0		1.055	612
671.5		631.6		1.063	
703.0		670.5	674.5	1.045	704
761.2	763.2	733.5		1.039	765
993.5		966.5		1.028	993
1250		1201.5	1216.5	1.034	1245
1295		1233.0		1.050	1280
1337	1465	1278.0	1414.5	1.041	1360

mass and ionic radius, the energies of external vibrations change, while the energies of internal vibrations of any complexes change insignificantly. In addition, as can be seen from Tables 1 and 2, the frequency position of external and internal vibrations of E modes in TbAl$_3$(BO$_3$)$_4$ is not separated by any significant interval as it was observed in ferroborates [13, 15, 16] and a number of other compounds. The assignment of the E mode 601.5 cm^{-1} (Table 1) to the external vibrations and 612.5 cm^{-1} (Table 2) to the internal vibrations was carried out on the basis of an analysis of the splitting of modes into TO and LO components and the characteristic behavior of the LO component at $\theta = 45°$.

Isomorphic substitution, as a rule, is used not only for separation into external and internal vibrations, but also for identification of the vibrational modes caused by vibrations of ions substituted by another one. In our case, in according to the group-theory analysis, $A_1 + 3E$ modes should be observed for vibrations of $3d$ metal ions [8, 13]. As you can see from the Table 1, the largest change in frequency by a factor of 1.434 is observed for the A_1 mode at 259.1 cm^{-1} in TbAl$_3$(BO$_3$)$_4$ [180.6 cm^{-1} in TbFe$_3$(BO$_3$)$_4$] upon substitution of aluminum for iron. Likewise, a similar picture is observed for two E modes: a factor of 1.405 for 224.7 cm^{-1} and a factor of 1.389 for 384.4 (TO) and 396.8 (LO) cm^{-1} in the Raman spectra of TbAl$_3$(BO$_3$)$_4$. It is more difficult to identify the third E mode of vibration of a $3d$ metal ion. This can be the 259.2 (TO) and 260.5 (LO) cm^{-1} mode in TbAl$_3$(BO$_3$)$_4$ which is observed with a change in frequency by a factor of 1.315 as a result of isomorphic substitution as well as the 302.2 cm^{-1} mode with a change in frequency by a factor of 1.311 (Table 1).

In addition to the discussed above A_1, A_2, and E modes, an additional line observed in the Raman spectrum can be assigned to the E mode at 630.0 cm^{-1}. This line is marked with a question in Fig. 2. Moreover, this line is observed in the scattering geometry with $\theta = 90°$ in polarization configurations $Y(XY)X$, $Y(XZ)X$, $Y(ZY)X$ and is not observed at $\theta = 45°$ in $Z(YY, XY, XZ, YZ)X$ (Fig. 2). Several crystals of this family have a monoclinic structure and some of them can have regions containing a monoclinic phase that is induced by the growth conditions [8]. At the same time, for the monoclinic phase, the additional A_2 and E lines appear in the transmission spectrum in the range of 200–400 cm^{-1} [8]. In our case, no additional lines are observed in the indicated energy range. But it is also impossible to say unequivocally that only $R32$ (D_3^7) phase is present in the studied crystal. This is due to the fact that the intensities of the E lines in the IR and Raman spectra can differ significantly. At the moment, there is no unambiguous interpretation of this additional line. It can be assumed that this line is observed in the Raman spectra taken near the growth face containing the regions with a monoclinic phase or some defects distorting the crystal lattice. In another scattering geometry, the Raman spectrum was taken from a point near the cut and polished face, i. e., inside the sample. In this case, no additional line (630.0 cm^{-1}) was observed (Fig. 2).

As seen from Fig. 2, in addition to the first order phonon spectrum and an additional phonon line registered at 5 K, we observed some broad lines that were not observed in ferroborates [13, 15, 16]. They are most clearly seen in the Raman spectrum obtained in the *ZZ*-polarization configuration (Fig. 2). In addition to single-particle phonon
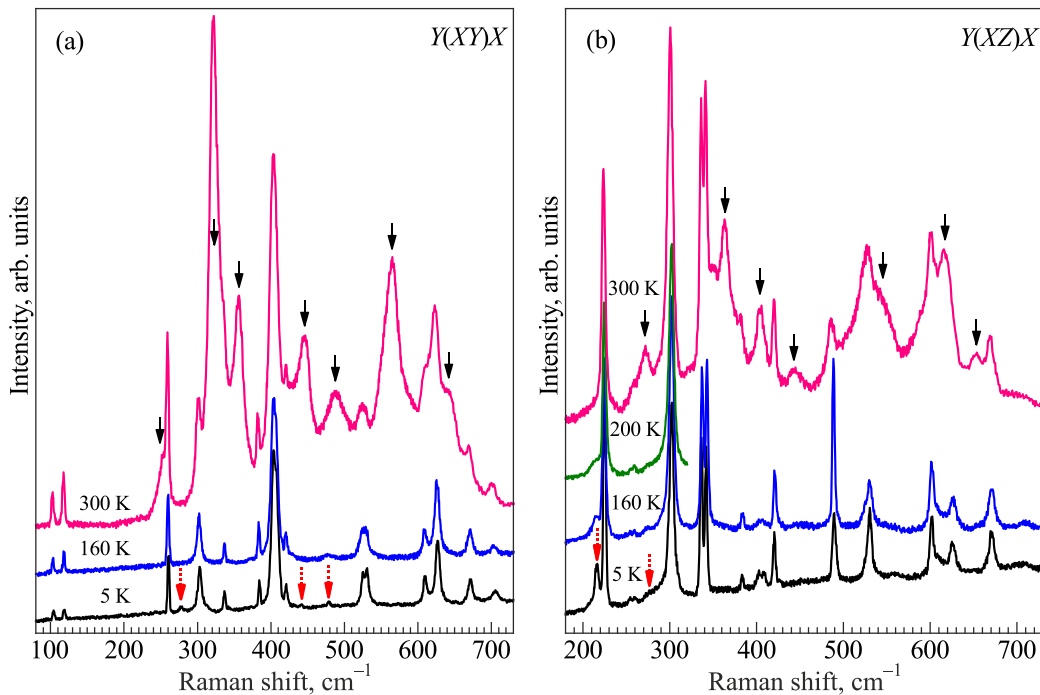

Fig. 3. The temperature evolution of the Raman spectra of the TbAl$_3$(BO$_3$)$_4$ single crystal in the different polarization geometries: (a) *Y(XY)X* and (b) *Y(XZ)X*; $\lambda_{exc} = 532$ nm (36 mW); the spectral resolution of 3.0 cm^{-1}.

excitations there can be observed lines related to electronic transitions within the main multiplet of Tb^{3+} and lines corresponding to two-particle processes in the same frequency range. The lines assigned to these two types of excitations, as a rule, have a width that is much wider than the width of the lines associated with single-particle phonon vibrations even at low temperatures. It is known that the intensity of the lines assigned to electronic transitions decreases with increasing temperature, while their width increases, and at some temperatures they are no longer observed. The intensity of the lines of two-particle excitations increases with increasing temperature.

Figure 3 shows the temperature evolution of the range of the Raman spectra in two polarization geometries: *Y(XY)X* and *Y(XZ)X*. As expected, the intensity of the lines associated with low-energy electronic transitions within the $^7F_6$ ground multiplet of Tb^{3+} decreases with increasing temperature [Figs. 3(a), 3(b)], while their width increases [Fig. 3(b)]. These lines are marked with dotted arrows in Figs. 3(a), 3(b). At the same time, when the temperature rises over ~ 200 K, the intense broad bands appear in the Raman spectra. The intensity of these lines may exceed the intensity of the phonon lines of the Raman spectrum. The appearance of these lines at room temperature was unexpected and ambiguous. It stimulated us to turn to the study of the luminescent features of the TbAl$_3$(BO$_3$)$_4$ crystal.

3.2. Luminescence properties of TbAl$_3$(BO$_3$)$_4$

Figure 4 shows the Raman spectrum and luminescence of TbAl$_3$(BO$_3$)$_4$ taken in the polarization geometry *Y(ZY)X* with excitation wavelength at λ_{exc} = 532 nm (18797 cm^{-1})

and 300 K in the energy range from 11800 to 20900 cm^{-1}. The excitation line is indicated by a vertical green bar in Fig. 4. The phonon anti-Stokes Raman scattering is observed in the energy range above the narrow excitation line. A group of broad bands is observed in the energy range of 20120–20750 cm^{-1}. The right inset in Fig. 4 shows a zoom of this group of lines in the different polarization configurations. The Raman spectrum as well as broad bands arising at high temperatures are observed in the range of 17000–18600 cm^{-1}. A band has a complex shape with anomalously high intensity was found in the region of 11800–16200 cm^{-1}. The power of the laser beam was attenuated by a neutral light filter down to about 1.2 mW to record this part of the spectrum. Also, the measured signal was divided by the coefficient presented in Fig. 4 to show the relationship between its intensity and the intensity of the Raman spectrum.

The high intensity of the measured signal indicates that we observe rather luminescence of TbAl$_3$(BO$_3$)$_4$ than Raman scattering in the region of 11800–16200 cm^{-1}. In order to test this scenario, the different excitation wavelengths were used. Figure 4 shows the spectrum (bottom curve) with excitation at 632.8 nm which is indicated in the red bar. The laser power equal to 30 mW was attenuated to ~ 1 mW as described above. As seen from Fig. 4, the spectra observed in the region of 11800–15800 cm^{-1} coincide in shape and are close in intensity at different wavelengths of the exciting light. This unambiguously indicates that the luminescence spectrum of TbAl$_3$(BO$_3$)$_4$ is observed in this energy range. The luminescence spectrum consists of a broad band and relatively narrow intense lines in the region
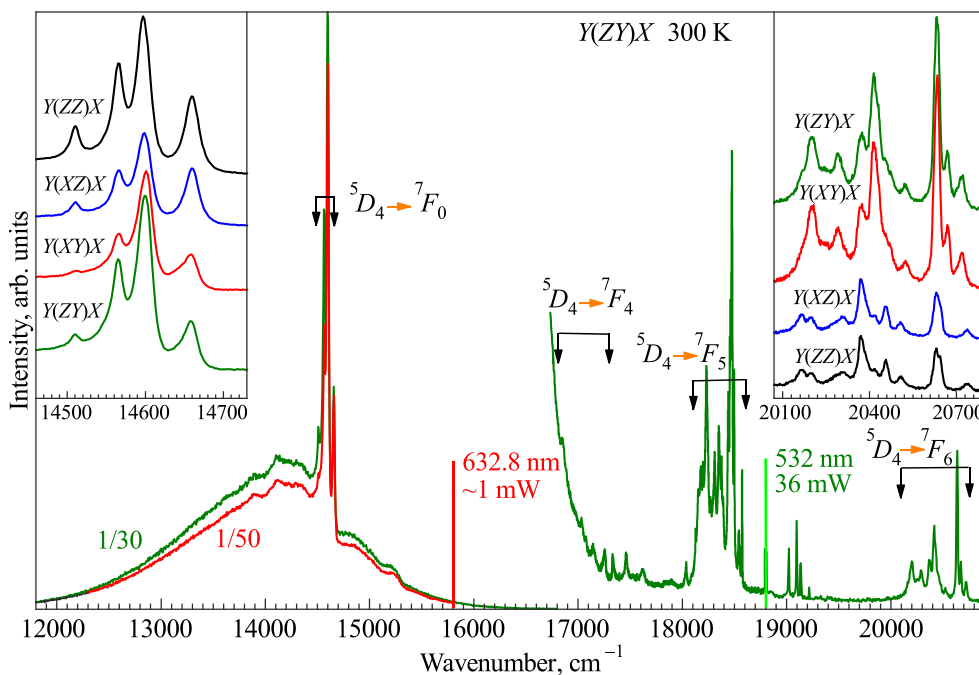

Fig. 4. The Raman spectra and luminescence of the TbAl$_3$(BO$_3$)$_4$ single crystal at 300 K; λ_{exc} = 532 nm (36 mW, ~ 1.2 mW (11800–16800 cm^{-1})) and λ_{exc} = 632.8 nm (~ 1 mW); the spectral resolution of 3.0 cm^{-1}.

of ~ 14600 cm^{-1}, which are shown in an enlarged scale in different polarization geometries in the left inset in Fig. 4.

It is known [6, 7] that Tb^{3+} doesn't have electronic levels in the region of ~ 14600 cm^{-1}. The appearance of luminescence in this region can be associated with the presence of impurities, for example, Nd. An analysis of the absorption spectra of TbAl$_3$(BO$_3$)$_4$ measured in the range of 11800–20900 cm^{-1} revealed only bands in the region of the $^5D_4$ multiplet (20634–20746 cm^{-1} at 77 K [6, 7]). The spectrum is shown in the present work also contains lines within the ~ 20600–20750 cm^{-1} energy region partially presented in the right inset in Fig. 4. Based on the previously published data [6, 7], the low-energy electronic levels of Tb^{3+} were obtained at 77 K: $^7F_0$ — 5994 cm^{-1}, $^7F_1$ — 5672–5794 cm^{-1}, $^7F_2$ — 5120–5424 cm^{-1}, $^7F_3$ — 4525–4691 cm^{-1}, $^7F_4$ — 3454–3775 cm^{-1}, $^7F_5$ — 2150–2426 cm^{-1}, $^7F_6$ — 0–472 см$^{-1}$. Analyzing these data, it is possible to determine the energy ranges of transitions (indicated by arrows in Fig. 4) from the excited $^5D_4$ multiplet to lower energy ones. It can be seen that in the energy range of 20100–20750 cm^{-1}, there are the bands associated with transitions from $^5D_4$ to both the ground level and thermally populated levels induced by splitting of the $^7F_6$ multiplet by the crystal field. The emission bands associated with the transitions from $^5D_4$ to $^7F_5$ and from $^5D_4$ to $^7F_4$ superimpose on the phonon Raman spectrum. Intense luminescence lines in the region of 14600 cm^{-1} are due to transitions from $^5D_4$ to $^7F_0$ (Fig. 4 and left inset in Fig. 4).

Here the question arises as to how luminescence is observed from the $^5D_4$ multiplet (20600–20750 cm^{-1}) under laser excitation by the line λ_{exc} = 532 nm (18797 cm^{-1}) and λ_{exc} = 632.8 nm (15803 cm^{-1}). The only explanation for those is the strong nonlinear properties of aluminum borates. Previously, nonlinear properties were investigated mainly in the YAl$_3$(BO$_3$)$_4$ and GdAl$_3$(BO$_3$)$_4$ crystals [1–3]. Indeed, in the present work, for TbAl$_3$(BO$_3$)$_4$, the decrease in the luminescence intensity by about four times was observed with a twofold decrease in the exciting laser power. Thus, we observe frequency doubling in the TbAl$_3$(BO$_3$)$_4$ crystal even at a relatively low power of the exciting light that is characteristic of nonlinear crystals. In doing so the laser excitation energies of ~ 15800 and ~ 18800 cm^{-1} are doubled up to ~ 31600 and ~ 37600 cm^{-1}, respectively. The doubled values of the excitation energy fall into the absorption region of aluminoborates [20]. Then the relaxation occurs to the $^5D_4$ levels and emission to the lower-lying levels of Tb^{3+} – $^7F_0$–$^7F_6$. The question remains, why the dominant part of the luminescence intensity falls on the transition from the excited $^5D_4$ multiplet not to the ground $^7F_6$, but to $^7F_0$ (~ 6000 cm^{-1}).

There is another question: why the $^5D_4$ multiplet does consist of three groups of lines while 4 bands are observed upon transition to the $^7F_0$ singlet? To answer this question, we analyzed the temperature evolution of the luminescence spectra in this region (Fig. 5). The spectra were obtained
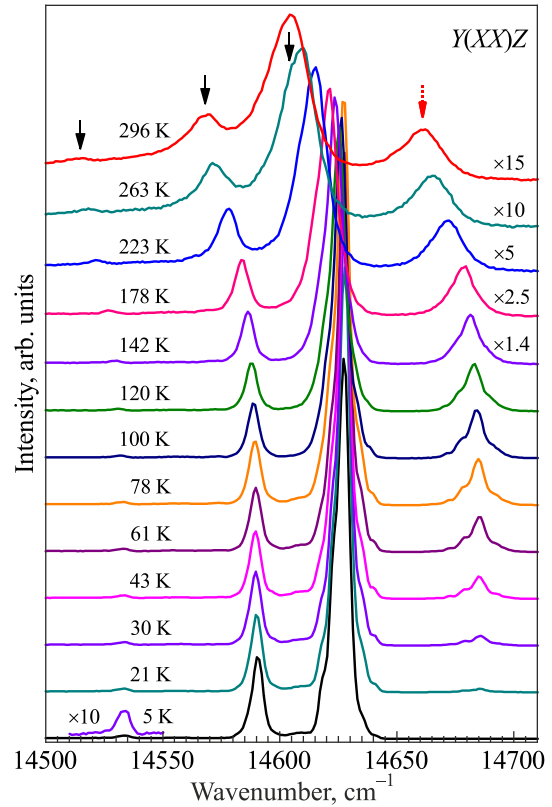

Fig. 5. The temperature evolution of the luminescence spectra of the TbAl$_3$(BO$_3$)$_4$ single crystal in the polarization geometry *Y(XX)Z*; λ_{exc} = 632.8 nm (~ 0.03 mW); the spectral resolution of 3.0 cm^{-1}.

with excitation at λ_{exc} = 632.8 nm (15803 cm^{-1}) and the spectral resolution of the spectrometer was 3 cm^{-1}. The luminescence intensity increased significantly with decreasing temperature therefore the laser radiation power was attenuated down to ~ 0.03 mW. Figure 5 shows three bands at low temperatures, as expected. With rising temperature over ~ 21 K, the ignition of the fourth higher-frequency band is observed. This band is assigned to the thermal population of some excitation. As you can see from Table 1, the only excitation observed in this a low-frequency region can be assigned to A_2 mode at 79 cm^{-1}. As the temperature rises, the luminescence intensity significantly decreases from the $^5D_4$ multiplet to $^7F_0$ (Fig. 5), at the same time, the bands associated with transitions from $^5D_4$ to $^7F_6$, $^7F_5$, $^7F_4$ ignite (Figs. 3, 4).

3.3. Electronic transitions of Tb^{+3} in the TbAl$_3$(BO$_3$)$_4$ single crystal

As noted above, several additional lines in addition to phonon modes are observed in the range of 200–500 cm^{-1} at 5 K (Figs. 2, 3). Some of them exhibit a temperature evolution characteristic to the electronic transitions. These lines are indicated with dotted arrows in Fig. 3. In addition to them, the luminescence lines assigned to the transitions from $^5D_4$ to $^7F_5$ fall into this energy range. These lines have low intensity in the spectra taken in the polarization con-

figurations *Y(XY)X* and *Y(XZ)X* at low temperatures, and they get more intense at room temperature (Fig. 3). To exclude the influence of luminescence lines on the spectrum of electronic transitions within the $^7F_6$ main multiplet of Tb^{3+}, the Raman spectra were recorded in the energy range of 200–500 cm^{-1} at λ_{exc} = 632.8 nm.

Figure 6 shows the regions of the Raman spectra in the range of low-energy electronic transitions of Tb^{3+}. The accumulation time of the spectra was several times longer than for the spectra shown in Fig. 3. As seen in Fig. 6, the lines previously assigned to electronic transitions of Tb^{3+} are observed both at λ_{exc} = 532 and 632.8 nm. The energies of electronic transitions within the $^7F_6$ main multiplet of Tb^{3+} at 5 K are presented in Table 3. The literature data obtained at 77 K by using other techniques have been added to Table 3 [6, 7]. As you can see from Table 3, the values of the energies of electronic transitions obtained by us at 5 K are slightly higher than the energies obtained at 77 K [6, 7] that indicates a normal temperature evolution.

The energies of the electronic levels of the $^5D_4$ multiplet can be obtained from the luminescence spectra measured at 300 K (Fig. 4 and left inset in Fig. 4). In the energy range of 20600–20750 cm^{-1}, there are bands associated with transitions from $^5D_4$ to the ground level. From the analysis
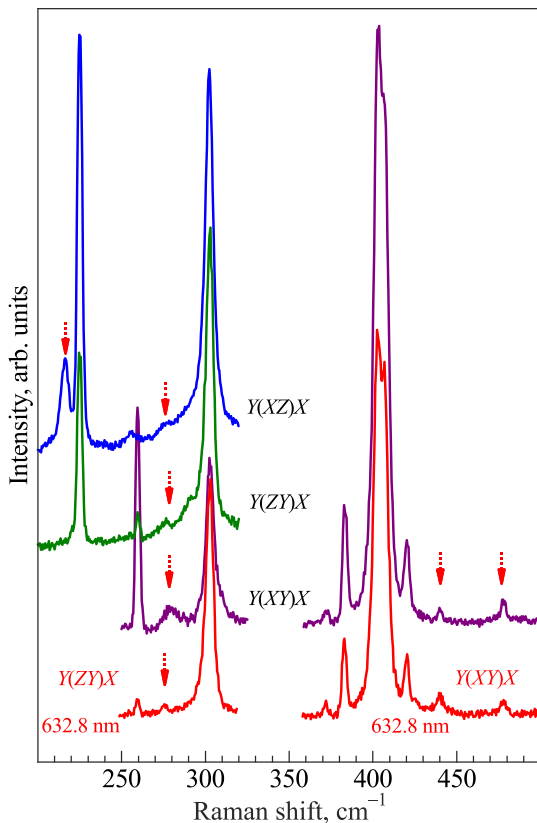
Table 3. The comparative analysis of the energy values (cm^{-1}) of the observed electronic transitions of Tb^{3+} in the $TbAl_3(BO_3)_4$ single crystal taken at 5 and 300 K and the literature data

Present work		[6]	[7]
5 K	300 K	77 K	77 K
216.5	213	210	217
276.0	271	272	271
279.5	280	275	275
440.1	429	434	436
478.0	469	472	472

of the values of the transition energies in the range of 20100–20600 cm^{-1}, it is possible to determine the energies of the thermally populated levels of the $^7F_6$ main multiplet (Table 3).

The energies of the $^5D_4$ electronic levels obtained from analysis of our results are: 20630 (30631), 20633 (30634), 20644 (30649), 20670 (30670), 20717 (30719), and 20737 (30746) cm^{-1}. They practically coincide with the values obtained at 77 K [7] which are presented in the brackets. This represents an absence of temperature evolution in the energy of the $^5D_4$ electronic levels. Therefore, the significant (~ 20 cm^{-1}) shift of the luminescence lines in the range of the transition from $^5D_4$ to $^7F_0$ (Fig. 5) reflects the temperature evolution of the $^7F_0$ level.

Conclusion

For the first time, Raman studies of the $TbAl_3(BO_3)_4$ single crystal were carried out in the frequency range of 3–1600 cm^{-1} and temperature interval of 5–300 K. Five of seven A_1 and all 19E phonon modes predicted by group-theory analysis for the crystal of given symmetry were observed. The splitting between LO and TO components of polar E phonons was determined by using the different polarization geometries. Three out of 12 A_2 modes forbidden in the Raman spectra were revealed. The comparison of the phonon spectrum of the studied crystal with the isomorphic $TbFe_3(BO_3)_4$ compound made it possible to identify vibrational modes with the involvement of the 3d metal ion.

The analysis of the luminescence spectrum measured in the energy region of 11800–21000 cm^{-1} at 300 K was performed. It was found that the most intense bands in the region of 14520–14680 cm^{-1} could be assigned to the electronic transitions $^5D_4 \rightarrow {}^7F_0$. Upon cooling, the intensity of the lines associated with these transitions increases. The intensity of the bands assigned to $^5D_4 \rightarrow {}^7F_6$, $^5D_4 \rightarrow {}^7F_5$ and $^5D_4 \rightarrow {}^7F_4$ transitions observed at room temperature is comparable to the intensity of the phonon bands in the Raman spectrum. With decreasing temperature, their intensity decreases. The observation of luminescence from the $^5D_4$ multiplet (20600–20750 cm^{-1}) at λ_{exc} = 632.8 nm (15803 cm^{-1}) and λ_{exc} = 532 nm (18797 cm^{-1}) indicates the nonlinear properties of the studied crystal.

Fig. 6. The Raman spectra of $TbAl_3(BO_3)_4$ taken in the different polarization configurations within main multiplet $^7F_6$ at 5 K; λ_{exc} = 532 nm (36 mW) and λ_{exc} = 632.8 nm (30 mW, bottom red spectra); the spectral resolution of 5.0 cm^{-1}.

The electronic structure of the ground multiplet $^7F_6$ of Tb^{3+} in the $TbAl_3(BO_3)_4$ single crystal was studied. For the first time, the experimental values of the energies of electronic transitions were obtained at 5 K from the analysis of the Raman spectra. The energies of the electronic levels of the $^7F_6$ and $^5D_4$ multiplets were determined at 300 K from the luminescence spectra. It's in good agreement with the previously published data obtained from the analysis of the optical spectra recorded at 77 K.

———

1. D. Jaque, *J. Alloys Compd.* **323–324**, 204 (2001).

2. Alain Brenier, Chaoyang Tu, Zhaojie Zhu, and Baichang Wu, *Appl. Phys. Lett.* **84**, 2034 (2004).

3. Xueyuan Chen, Zundu Luo, D. Jaque, J.J. Romero, J. Garcia Sole, Yidong Huang, Aidong Jiang and Chaoyang Tu, *J. Phys.: Condens. Matter* **13**, 1171 (2001).

4. V. A. Bedarev, M. I. Paschenko, M. I. Kobets, K. G. Dergachev, E. N. Khatsko, S. L. Gnatchenko, A. A. Zvyagin, T. Zajarniuk, A. Szewczyk, M.U. Gutowska, L. N. Bezmaternykh, and V.L. Temerov, *Fiz. Nizk. Temp.* **41**, 687 (2015) [*Low Temp. Phys.* **41**, 534 (2015)].

5. M. I. Pashchenko, V. A. Bedarev, D. M. Merenkov, O. M. Bludov, V. O. Pashchenko, S. L. Gnatchenko, T. Zajarniuk, A. Szewczyk, L. N. Bezmaternykh, and V. L. Temerov, *Fiz. Nizk. Temp.* **43**, 789 (2017) [*Low Temp. Phys.* **43**, 631 (2017)].

6. C. Gorller-Walrand, P. Vandevelde, I. Hendrickx, P. Porcher, and J. C. Krupa, *Inorg. Chim. Acta* **139**, 277 (1987).

7. I. Couwenberg, K. Binnemans, H. De Leebeeck, and C. Gorller-Walrand, *J. Alloys and Comp.* **274**, 157 (1998).

8. E. A. Dobretsova, E. Yu. Borovikova, K. N. Boldyrev, V. S. Kurazhkovskaya, and N. I. Leonyuk, *Optics and Spectroscopy* **116**, 77 (2014).

9. H. R. Xia, L. X. Li, J. Y. Wang, W. T. Yu, and P. Yang, *J. Raman Spectrosc.* **30**, 557 (1999).

10. Aleksandr S. Oreshonkov, Evgenii M. Roginskii, Nikolai P. Shestakov, Irina A. Gudim, Vladislav L. Temerov, Ivan V. Nemtsev, Maxim S. Molokeev, Sergey V. Adichtchev, Alexey M. Pugachev, and Yuriy G. Denisenko, *Materials* **13**, 545 (2020).

11. L. N. Bezmaternykh, V. L. Temerov, L. A. Gudim, and N. A. Stolbovaya, *Crystall. Rep.* **50**, Suppl. 1, 97 (2005).

12. Saehwa Chong, Brian J. Riley, Zayne J. Nelsona and Samuel N. Perry, *Acta Cryst. E* **76**, 339 (2020)

13. D. Fausti, A. A. Nugroho, P. H. M. van Loosdreht, S. A. Klimin, and M. N. Popova, *Phys. Rev. B* **74**, 024403 (2006).

14. H. Poulet, J.-P. Mathieu, *Vibrational Spectra and Crystal Symmetry*, Mir, Moscow (1973) [H. Poulet et J.-P. Mathieu, *Spectres de Vibration et Symetrie des Cristaux*, Cordon and Breach, Paris (1970)].

15. A. V. Peschanskii, A. V. Yeremenko, V. I. Fomin, L. N. Bezmaternykh, and I. A. Gudim, *Fiz. Nizk. Temp.* **40**, 219 (2014) [*Low Temp. Phys.* **40**, 171 (2014)].

16. A. V. Peschanskii, V. I. Fomin, and I. A. Gudim, *Fiz. Nizk. Temp.* **42**, 607 (2016) [*Low Temp. Phys.* **42**, 475 (2016)].

17. S. M. Shapiro and J. D. Axe, *Phys. Rev. B* **6**, 2420 (1972).

18. W. Hayes and R. Loudon, *Scattering of Light by Crystals*, J.Wiley and Sons, New York (1978).

19. Yukio Hinatsu, Yoshihiro Doi, Kentaro Ito, Makoto Wakeshima, and Abdolali Alemi, *J. Solid State Chem.* **172**, 438 (2003).

20. K.N. Boldyrev, M.N. Popova, M. Bettinelli, V.L. Temerov, I.A. Gudim, L.N. Bezmaternykh, P. Loiseau, G. Aka, and N.I. Leonyuk, *Opt. Mater.* **34**, 1885 (2012).

———

Спектроскопічне дослідження монокристалу $TbAl_3(BO_3)_4$: раманівське розсіювання світла та люмінесценція

A. V. Peschanskii, A. Yu. Glamazda, I. A. Gudim

Досліджено коливальні та люмінесцентні властивості монокристалу $TbAl_3(BO_3)_4$ в інтервалі температур 5–300 К. В раманівських спектрах монокристалу виявлено 5 з 7 A_1 та всі, що передбачено теоретико-груповим аналізом, E фононні моди. Визначено енергію розщеплення між LO й TO компонентами полярних E фононів. В спектрах люмінесценції, в діапазоні 14520–14680 см$^{-1}$, виявлено групу інтенсивних смуг, яка може бути пов'язана з електронним переходом $^5D_4 \to {}^7F_0$. При нагріванні інтенсивність цих смуг зменшується. У той же час при кімнатній температурі спостерігаються смуги, які можуть бути пов'язані з $^5D_4 \to {}^7F_6$, $^5D_4 \to {}^7F_5$ та $^5D_4 \to {}^7F_4$ переходами, інтенсивність яких порівнянна з інтенсивністю смуг в раманівському спектрі $TbAl_3(BO_3)_4$. Спостереження люмінесценції з рівня $^5D_4$ (20600–20750 см$^{-1}$) при збудженні $\lambda_{exc} = 632,8$ нм (15803 см$^{-1}$) та $\lambda_{exc} = 532$ нм (18797 см$^{-1}$) свідчить про сильні нелінійні властивості досліджуваного кристалу. Методом раманівської спектроскопії досліджено структуру основного мультиплету $^7F_6$ іону Tb^{+3} в монокристалі $TbAl_3(BO_3)_4$ при 5 К. З аналізу спектрів люмінесценції визначено значення енергій електронних рівнів мультиплетів $^7F_6$ та $^5D_4$ при 300 К.

Ключові слова: $TbAl_3(BO_3)_4$, коливальний спектр, електронні переходи, раманівська спектроскопія, люмінесценція.